

Nonlinear dynamic analysis for large-span single-layer reticulated shells subjected to wind loading

Yuan-Qi Li[†]

Department of Building Engineering, Tongji University, Shanghai 200092, China

Yukio Tamura[‡]

Wind Engineering Research Center, Tokyo Polytechnic University, Atsugi 243-0297, Japan

(Received September 15, 2003, Accepted November 10, 2004)

Abstract. Wind loading is very important in structural design of large-span single-layer reticulated shell structures. In this paper, a geometrically nonlinear wind-induced vibration analysis strategy for large-span single-layer reticulated shell structures based on the nonlinear finite element method is introduced. According to this strategy, a computation program has been developed. With the information of the wind pressure distribution measured simultaneously in the wind tunnel, nonlinear dynamic analysis, including dynamic instability analysis, for the wind-induced vibration of a single-layer reticulated shell is conducted as an example to investigate the efficiency of the strategy. Finally, suggestions are given for dynamic wind-resistant analysis of single-layer reticulated shells.

Keywords: large-span single-layer reticulated shells; wind-induced vibration; nonlinear dynamic analysis; dynamic stability.

1. Introduction

Single-layer reticulated shells are widely used as a spatial structural system with medium or large spans. For such a structural system, stability is a serious, even dominant problem, and usually the sensitivity of such shells to external load distribution is evident (Gioncu 1995). Considering the random characteristics of wind load distribution, wind-resistant analysis of these shells should be well considered in structural design, especially for the shells with large spans. In most cases, it should be paid more attention to than earthquake action. A series of wind tunnel tests had been conducted by Uematsu, *et al.* (1997) and (2001), to investigate the wind load distributions on the spherical shell models supported on the cylinders with different heights, and the wind-induced dynamic responses, including the displacements of joints and the internal force of elements, of the corresponding single-layer reticulated domes were also analyzed based on the proper orthogonal decomposition (POD) technique. However, non-linear behavior and stability problem of the domes

[†] Associate Professor, Formerly, Research Associate of Wind Engineering Research Center, Tokyo Polytechnic University, Corresponding author, E-mail: liyq@mail.tongji.edu.cn

[‡] Professor

under wind load were not concerned in these investigations. At present, usually equivalent static methods are used in the structural design with wide discussions (Solari 1990, Xie, *et al.* 2000, Li 2002, Uematsu, *et al.* 2002). Unfortunately, it is difficult to estimate a suitable equivalent static wind load so that the effect of the fluctuating component of wind on structural behavior, especially on structural stability, can be well estimated. For some large-scale and important structures, an exact dynamic analysis is still necessary, at least as a final investigation on the dynamic effect of wind load in structural design process.

Up to now, although great progress has been made on the techniques for static stability analysis, and many research studies have been done for nonlinear dynamic analysis, dynamic stability analysis is still a challenge for the spatial structures, such as the definition and the criteria for determining dynamic instability, the techniques for dynamic stability analysis, and even the natural characteristics of such phenomenon (Li and Shen 2001, Abedi 2002, etc.). Further research is necessary on this topic, especially on the analysis techniques for practical use.

In this paper, through an analogical analysis between the nonlinear dynamic analysis equations and the nonlinear static formula considering the updating technique of large deformation, a practical approach is introduced for geometrically nonlinear dynamic analysis considering stability problem, and a program based on the approach has been developed. Based on the wind tunnel tests of a rigid spherical model, wind pressure distribution was measured simultaneously, and expanded to the whole surface of the shell using the proper orthogonal decomposition (POD) method. Then, wind induced vibration analysis, including dynamic instability analysis, of a corresponding K6-12 type single-layer reticulated shell is carried out as an example to investigate the efficiency of the theory and the program. Finally, suggestions are given for the dynamic wind-resistant analysis of single layer reticulated shells, especially for the stability problem.

2. Geometrically nonlinear dynamic analysis

Based on the theory of the nonlinear finite element (FEM) method, the nonlinear vibration equations for single-layer reticulated shells subjected to wind load are expressed as follows:

$$[M]\{\ddot{U}_t\} + [C]\{\dot{U}_t\} + [K]\{U_t\} = (\{F_D\} + \{F_L\}) + \{F_w(t)\} = \{P_t\} \quad (1)$$

where, $[M]$ is the mass matrix; $[C]$ is the damping matrix; $[K]$ is the structural nonlinear stiffness matrix; $\{U\}$, $\{\dot{U}\}$ and $\{\ddot{U}\}$ are the displacement, the velocity and the acceleration vectors, respectively; $\{F_D\}$ and $\{F_L\}$ are the dead load and the live load vectors; $\{F_w(t)\}$ is the external dynamic load vector; and $\{P_t\}$ is the total external time-series load vector.

Usually, a concentrated mass matrix is used in dynamic analysis of reticulated shell structures, since it is much simple and the accuracy is acceptable in comparison with the consistent mass matrix.

Regarding the damping matrix, it cannot be generated as the same as the mass or stiffness matrix from the corresponding matrix of each element. Usually, a proportional damping matrix is assumed to approximately reflect the energy dissipation in the actual structures, such as the widely used Rayleigh damping:

$$[C] = c_0[M] + c_1[K] \quad (2)$$

where $c_0 = 2\omega_1\xi_1 - c_1\omega_1^2$ and $c_1 = \{2(\omega_1\xi_1 - \omega_2\xi_2)\} / \{\omega_1^2 - \omega_2^2\}$. ω_i and ξ_i is the circular frequency

and the critical damping ratio corresponding to the i -th vibration mode, respectively, $i=1, 2$.

It has been pointed out that the Rayleigh damping is just a theoretical assumption in many cases with an obvious feature that the decline of the higher-order vibration modes will be much faster than that of the lower-order vibration modes. So the values of c_0 and c_1 are usually based on the low-order vibration modes. In fact, to a certain structural analysis, they could be determined suitably based on the damping characteristics of a corresponding typical structure, since the Rayleigh constants are dominantly depend on the energy dissipation characteristics of the materials.

For the stiffness matrix of each element, the Oran beam-column theory (Oran 1973) is suitable and efficient for the nonlinear elements whose internal forces are axial force dominantly (Li, *et al.* 1997).

To solve Eq. (1), the Newmark β method are often used with the following assumptions as

$$\{\dot{U}_{t+\Delta t}\} = \{\dot{U}_t\} + [(1-\delta)\{\ddot{U}_t\} + \delta\{\ddot{U}_{t+\Delta t}\}]\Delta t \quad (3)$$

$$\{U_{t+\Delta t}\} = \{U_t\} + \{\dot{U}_t\}\Delta t + \left[\left(\frac{1}{2} - \alpha\right)\{\ddot{U}_t\} + \alpha\{\ddot{U}_{t+\Delta t}\}\right]\Delta t^2 \quad (4)$$

where α and δ are the coefficients, $\delta \geq \frac{1}{2}$ and $\alpha \geq \frac{1}{4}\left(\frac{1}{2} + \delta\right)^2$.

At $t+\Delta t$, the equilibrium equations corresponding to Eq. (1) can be rewritten as:

$$[M]\{\ddot{U}_{t+\Delta t}\} + [C]\{\dot{U}_{t+\Delta t}\} + [K]\{U_{t+\Delta t}\} = \{P_{t+\Delta t}\} \quad (1a)$$

Substituting Eq. (3) and Eq. (4) in Eq. (1a), it can be obtained that

$$[\bar{K}]\{U_{t+\Delta t}\} = \{\bar{P}_{t+\Delta t}\} \quad (5)$$

where,

$$[\bar{K}] = [K] - (a_0[M] + a_1[C]) \quad (6)$$

$$\{\bar{P}_{t+\Delta t}\} = \{P_{t+\Delta t}\} + [M](a_0\{U_t\} + a_2\{\dot{U}_t\} + a_3\{\ddot{U}_t\}) + [C](a_1\{U_t\} + a_4\{\dot{U}_t\} + a_5\{\ddot{U}_t\}) \quad (7)$$

$[\bar{K}]$ is the equivalent stiffness matrix; $\{\bar{P}_{t+\Delta t}\}$ is the equivalent loading vector; and $a_0 = \frac{1}{\alpha\Delta t^2}$,

$$a_1 = \frac{\delta}{\alpha\Delta t}, a_2 = \frac{1}{\alpha\Delta t}, a_3 = \frac{1}{2\alpha} - 1, a_4 = \frac{\delta}{\alpha} - 1, \text{ and } a_5 = \frac{\Delta t}{2}\left(\frac{\delta}{\alpha} - 2\right).$$

Here, Eq. (5) can be called “the nonlinear equivalent static equilibrium equations” for the nonlinear dynamic analysis of single-layer reticulated shells.

On the other hand, the nonlinear equilibrium equations in static analysis are expressed as

$$[K]_{i-1}\{U\}_i = \{P\} \quad (8)$$

With a proportional loading strategy, Eq. (8) can be rewritten as

$$[K_T]_{i-1}\{\Delta U\}_i = \Delta\lambda_i\{P\} \quad (9)$$

where $\Delta\lambda$ is the loading incremental parameter, and the limit value of the total loading increment parameter λ , λ_{cr} , can be used to represent the limit load-carrying capacity of structures.

With a comparison of Eq. (5) to Eq. (8), it can be found that the nonlinear equivalent static equilibrium equations at $t+\Delta t$ are similar to the nonlinear static equilibrium equations. Thus, the same methods, the arc-length method, to solve the nonlinear equivalent static equilibrium equations of Eq. (8) can be used to solve the nonlinear equivalent static equilibrium equations of Eq. (5).

To each time interval Δt , Eq. (5) can be written in an incremental form. This is, at the initial iterative step of the i -th incremental step, it can be expressed as

$$[K]_{i-1}\{\Delta U_{t+\Delta t}^1\}_i = (\Delta\lambda^1)_i\{\bar{P}_{t+\Delta t}\}_{i-1} \quad (10)$$

where,

$$[K]_{i-1} = [K_T]_{i-1} + (\Delta\lambda^1)_i(a_0[M] + a_1[C]) \quad (11)$$

$$\{\bar{P}_{t+\Delta t}\}_{i-1} = \{P_{t+\Delta t}\} - (a_0[M] + a_1[C])\{U_{t+\Delta t}\}_{i-1} \quad (12)$$

$(\Delta\lambda^j)_i$ is the loading incremental parameter at the j -th iterative step of the i -th incremental step.

Since the equivalent loading reference vector $\{\bar{P}_{t+\Delta t}\}$ is different at each iterative step, $(\Delta\lambda^j)_i$ will be modified in each iterative step, which can be called “a dynamic loading incremental parameter” (Li and Shen 2001).

A nonlinear analysis technique combining the Spherical Arc-Length method (or named as the Arc-Length-Crisfield method) with Riks-Wempner Normal method has been proven efficient for such structures with a steady ability (Li, *et al.* 1997). In this paper, this method was used.

In using the Spherical Arc-Length method combined with the Riks-Wempner Normal method, the initial loading incremental parameter at each incremental step is calculated as

$$|(\delta\lambda^0)_i| = \sqrt{\frac{(\Delta l_0)_i^2 - \{\delta q^0\}_i^T \{\delta q^0\}_i}{\{\bar{P}_{t+\Delta t}\}_{i-1}^T \{\bar{P}_{t+\Delta t}\}_{i-1}}} \quad (13)$$

And the controlling equation for the arc-length increments is given by Li and Shen (1997):

$$(\Delta l_0)_i = \beta_\varepsilon \beta \frac{\Delta \bar{S}_p}{|\Delta S_{pi}|} \sqrt{\frac{N_1}{N_2}} (\Delta l_0)_{i-1} \quad (14)$$

where N_1 is the number of the iterative steps for optimum, generally it equals 2. N_2 is the number of the iterative step in the last incremental step, but not bigger than 10. $\Delta \bar{S}_p$ is the pre-determined increment of the current stiffness parameter, usually in a range of 0.05~0.1; β is selected from 0.5~0.1, with a higher value taken for greater nonlinear degree and vice versa, generally it equals 0.8. $\beta_\varepsilon = \{\log_{10} \varepsilon_{i-1}\} / \{\log_{10} \varepsilon_0\}$, and it will equals 0.1 if $\varepsilon_{i-1} > 0.1$. ε_{i-1} is the convergent precision in the last incremental step, and ε_0 is the pre-determined convergent precision.

A new simple criterion for determining the sign of the initial loading incremental parameter presented by Li and Shen (1997), is used in this paper as:

$$(\delta\lambda^0)_i = \begin{cases} (-1)^n \text{sign}(S_p) |(\delta\lambda^0)_i| & (S_p \neq 0) \\ -\text{sign}((\delta\lambda^0)_{i-1}) |(\delta\lambda^0)_i| & (S_p = 0) \end{cases} \quad (15)$$

where S_p is the current stiffness parameter of the structures, and n is the number of the snapping back points before the current step in the equilibrium path.

3. Computational program and numerical example

According to the above strategy, a nonlinear dynamic analysis program considered the updating of large deformation has been developed by the authors. As a classic numerical example in stability analysis, William's Toggle was analyzed in this paper to check the efficiency of the program, as shown in Fig. 1. In the static stability analysis, totally four elements and two elements were used to check the efficiency of the Oran beam-column element for reticulated shells. Fig. 2(a) and Fig. 2(b) give the curves of the load P vs. the deformation at apex A, δ_A , and load P vs. the horizontal pushing force H , respectively. These results are consistent with other researchers' work (Chrescielewski and Schmiot 1985, etc.). At the same time, the results obtained by using only two elements is almost as the same as that by using four elements, which shows the efficiency of the Oran beam-column element theory in nonlinear analysis for reticulated shell structures.

With a mass of 15.0 kg at the apex A, nonlinear dynamic analysis under a normalized El-Centro

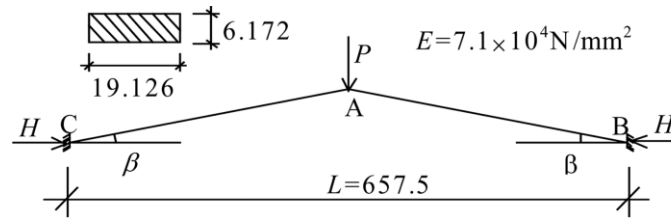


Fig. 1 William's Toggle ($0.5Lt\beta = 9.804$ mm, unit: mm)

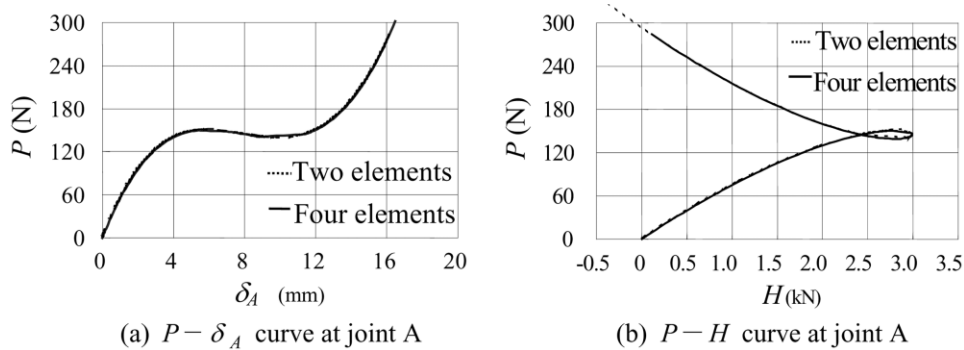


Fig. 2 Results from static stability analysis

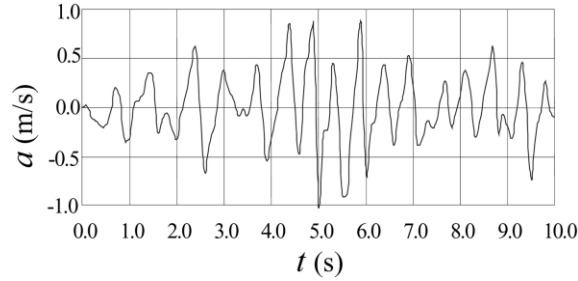


Fig. 3 A segment of normalized El-Centro earthquake wave in Z direction

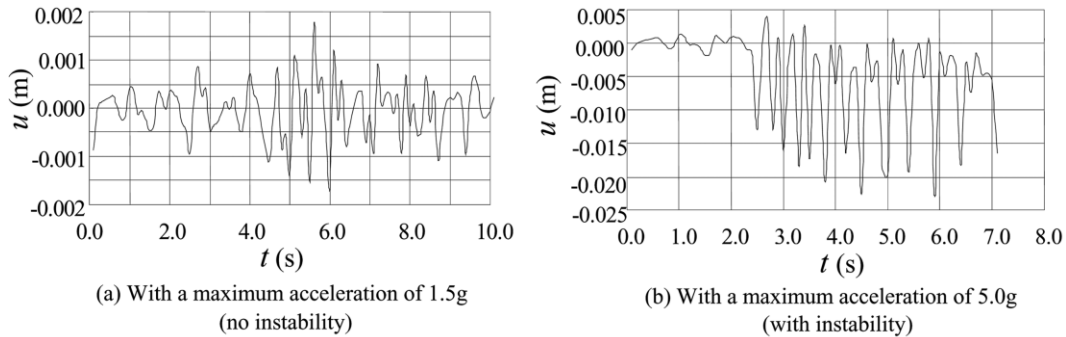


Fig. 4 Time series results of the vertical displacement at point A

earthquake wave in Z direction, as shown in Fig. 3, was conducted. Considering the maximum of the acceleration values of the normalized El-Centro earthquake wave as 1.5 g (without instability) and 5.0 g (with instability), respectively, the time-series results of the vertical displacement at point A are given in Fig. 4. Compared to the static instability curve in Fig. 2(b), it was found from Fig. 4(a) and Fig. 4(b) that, with a maximum acceleration of 1.5 g, no dynamic instability phenomenon occurred, and it is a normal nonlinear dynamic analysis. However, if the maximum acceleration increased up to 5.0 g, the dynamic instability occurred several times and led to a final diverge of the computation. It should be pointed out that, in the nonlinear static analysis, downward displacement is defined as the positive value, while in the nonlinear dynamic analysis, upward displacement is defined as positive.

4. Wind-induced vibration analysis for single-layer reticulated shells

4.1. Analysis model

A Kiewitt-type K6-12 single-layer reticulated spherical shell was chosen as the analysis model in this paper, as shown in Fig. 5. The span $L = 120$ m, and the rise $f = 40$ m. The sections of all elements in the model were assumed to be 200 mm diameter tubes with 8 mm thickness ($\phi 200 \times 8$ mm). All the joints on the bottom of the shell model were assumed fixed for all the six degree-of-freedom.

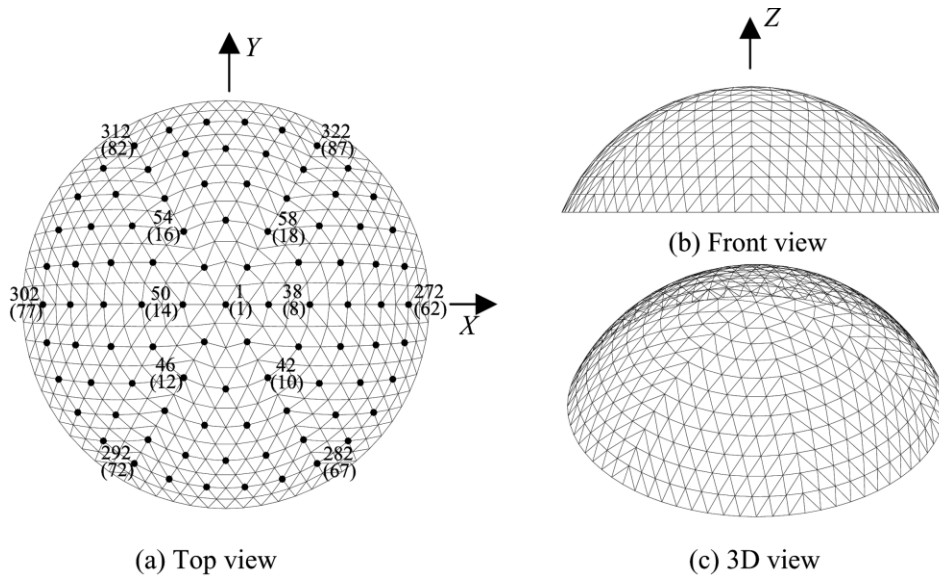


Fig. 5 Analysis model: A k6-12 single-layer reticulated spherical shell

4.2. Wind tunnel tests and results

In order to know the characteristics of the wind load distribution on the spherical analysis model, wind tunnel tests on a scaled model of the spherical shell according to the length scale in the wind tunnel, 1:400, had been conducted in the Boundary Layer Wind Tunnel (BLWT) of Wind Engineering Research Center, Tokyo Polytechnic University (WERC, TPU). It is a new open-circuit, low-speed boundary layer wind tunnel with a test section of 1.8 m high and 2.2 m wide. With the

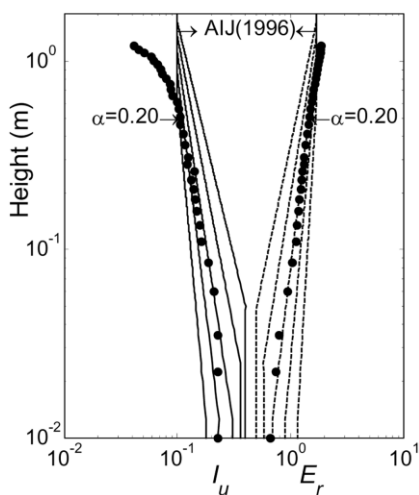


Fig. 6 Wind profiles

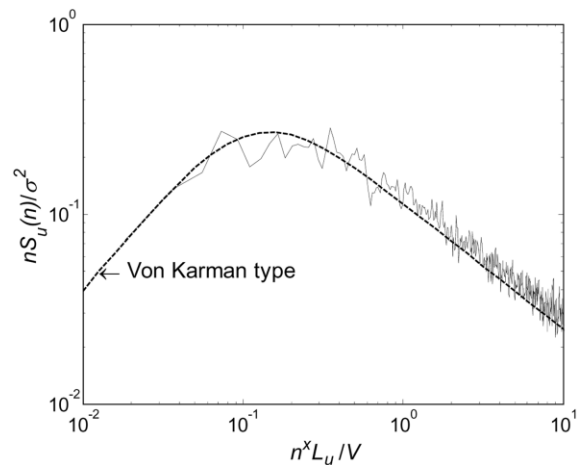


Fig. 7 Longitudinal PSD



Fig. 8 Picture of the wind tunnel test

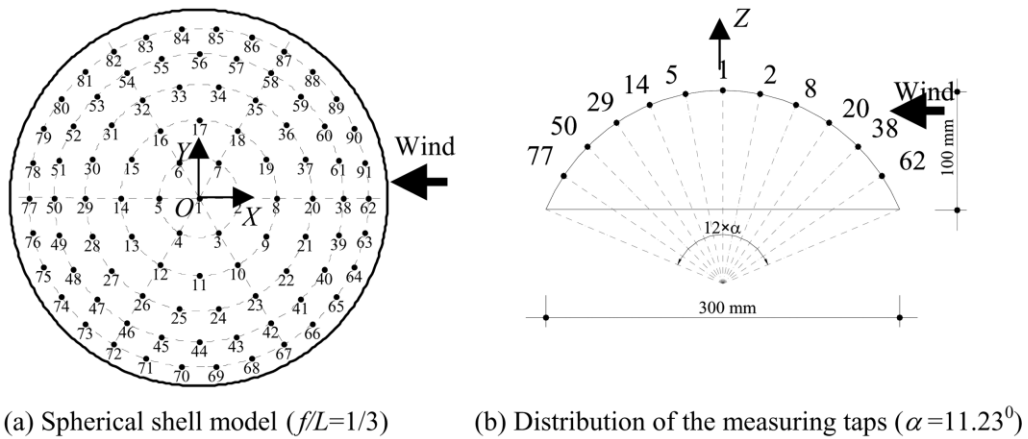
(a) Spherical shell model ($f/L=1/3$)(b) Distribution of the measuring taps ($\alpha=11.23^\circ$)

Fig. 9 The spherical shell model for wind tunnel tests and numbering of the measuring taps

widely-used spire-roughness technique, the wind profile corresponding to Terrain type III ($\alpha=0.20$) were simulated successfully (Li, *et al.* 2002), as shown in Fig. 6. In Fig. 6, the continuous lines without marks are based on Architectural Institute of Japan, AIJ, $E_r=U(z)/U_{10}^H$, which is the vertical distribution coefficient of windspeed in the flat uniformly rough (FUR) terrain, U_{10}^H is the windspeed at 10 m high above Terrain type II. Fig. 7 gives the longitudinal power spectral density (PSD) distribution of wind speed measured in the wind tunnel, which shows a good consistency with well-established Von Karman expression (1948). Fig. 8 shows a picture of the wind tunnel tests. Fig. 9 gives the size of the spherical shell model and the distribution of the measuring taps on its surface. As usual, wind speed and corresponding velocity pressure at the height of the apex of the shell model are taken as the reference wind speed and the reference pressure for calculating wind pressure coefficients. In addition, the test wind speed was about 10 m/s.

Fig. 10 gives the measured results of the mean and the fluctuating wind pressure coefficient

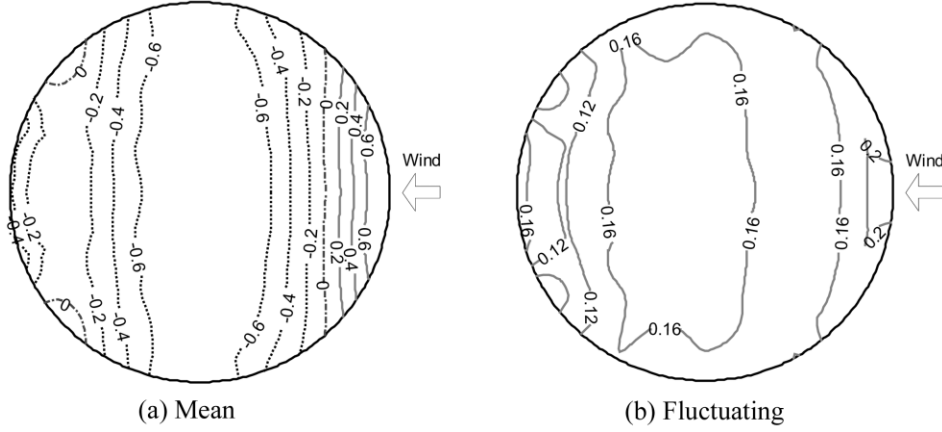


Fig. 10 Distribution of mean and fluctuating wind pressure coefficients

distributions. From Fig. 10 it was found that most area of the shell surface has suction pressure except for a small part in the windward side with positive pressure.

4.3. Expanding time-series wind pressure data

For single-layer reticulated shells, it is necessary to expand the measured mean or fluctuating wind pressure data of the limited measuring points to all the structural nodes on the surface of shell in order to conduct a static or dynamic structural analysis, since the effect of load distribution is very important, especially for static or dynamic stability analysis.

For the mean and the fluctuating wind pressure distribution, they can be expanded by numerical interpolation simply. However, it is not acceptable to get the time-series data of wind pressure at each node in the same way. Using the obtained orthonormal eigenvectors by the Proper Orthogonal Decomposition (POD) method as a coordinate system of the measured wind pressure field, expanding the wind pressure data to each point on the whole surface of the model based on the results from the wind tunnel test can be carried out for a dynamic analysis of its corresponding prototype structure conveniently within an acceptable error (Tamura, *et al.* 1999, Uematsu, *et al.* 1997 and 2001). By utilizing the orthogonality of the eigenvectors obtained by proper orthogonal decomposition as the M deterministic coordinates, the expanded fluctuating wind pressure field can be expressed as

$$p_i^e(t) = \sum_{m=1}^M a_m(t) \phi_{mi}^e \quad (16)$$

where, $\{\phi_m^e\}$ is the m -th expanded orthonormal eigenvector with n dimension, $m = 1, 2, \dots, M$, and $i = 1, 2, \dots, n$, and n is the number of nodes in the analysis model. $a_m(t)$ is the m -th principal coordinate given by

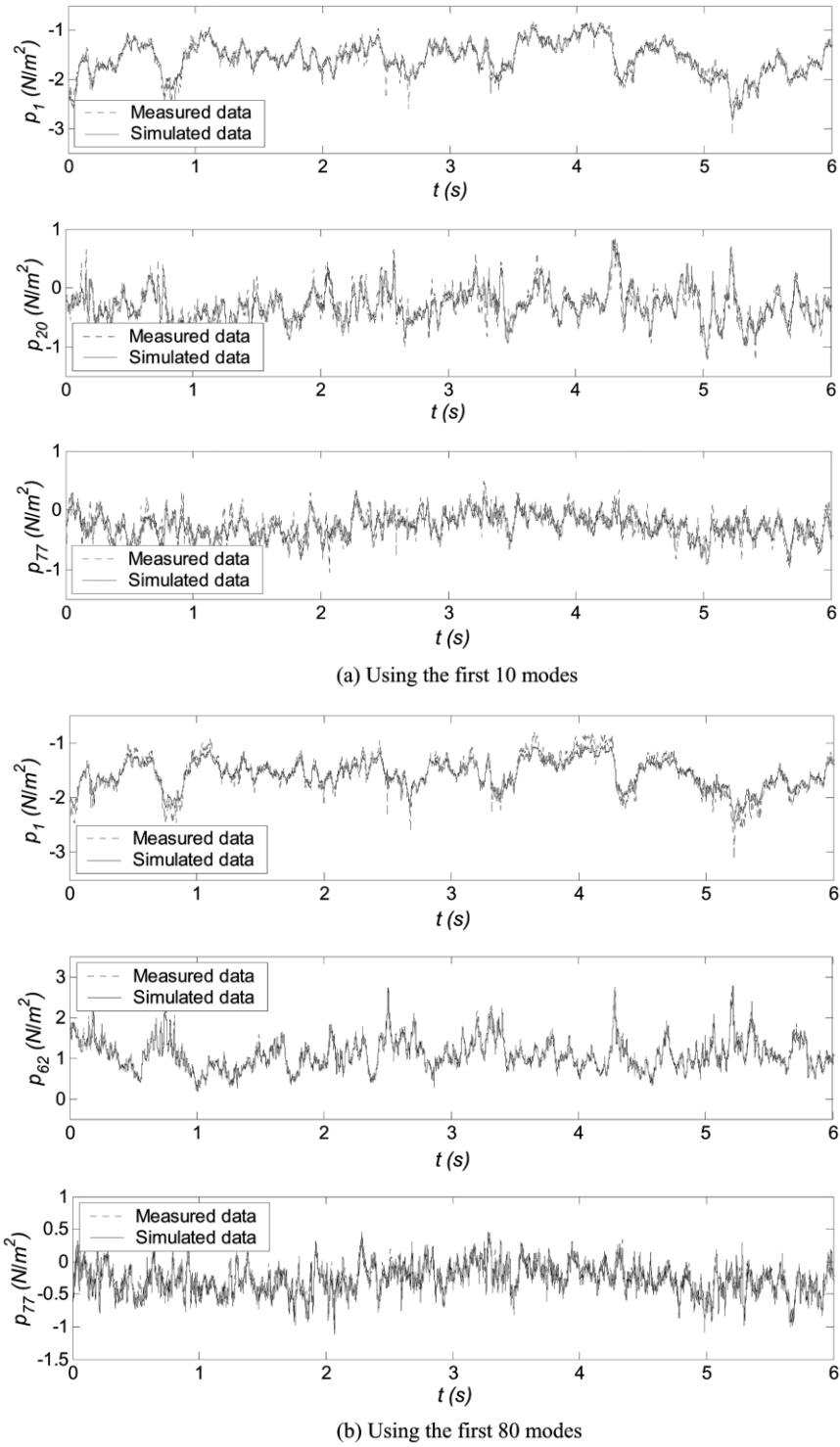


Fig. 11 Comparison of the reconstructed fluctuating wind pressures with the measured results

$$a_m(t) = \frac{\sum_{i=1}^N p_i(t) \phi_{mi} \Delta s_i}{\sum_{i=1}^N \phi_{mi}^2 \Delta s_i} \quad (17)$$

where, $p_i(t)$ is the measured wind pressure data at point i , $i = 1, 2, \dots, N$, N is the number of measuring points; $\{\phi_{mi}\}$ is the original m -th orthonormal eigenvector obtained from the proper orthogonal decomposition of the correlation coefficients matrix of the measured wind pressure field; Δs_i is the representative area at point i .

Fig. 11 gives a comparison of the reconstructed results of wind pressure using the first ten modes and the first 80 modes, respectively, with the measured results in the wind tunnel.

From Fig. 11 it was found that, for the reconstructed data of the points near to the apex of the spherical shell (e.g., Point 1), the results from the first ten modes and from the first 80 modes are almost the same, while for the reconstructed data of the points near to the bottom of the shell model, especially the points on the leeward side (e.g., Point 77), the results from the first ten modes and from the first 80 modes are really different, in which the latter has a much better consistency with the measured results. This also means that the first several modes are representative of total distribution of wind pressure distribution on the surface, while the other high-order modes are just helpful to the local distribution. In this case, in order to get acceptable expanded results, more than the first 20 modes should be considered with a cumulative contribution of the modes near 90%.

4.4. Nonlinear dynamic analysis

Using the nonlinear finite element program developed by the authors, nonlinear wind-induced vibration time-history analysis for the single-layer reticulated spherical shell under the measured wind load distribution was conducted. Fig. 12 gives a comparison between the nonlinear and the linear dynamic analysis results when the total loading increment parameter $\lambda = 6.0$ under a combination of wind load and dead load, in which the continuous lines are corresponding to the nonlinear dynamic analysis using the program developed by the authors, and the dashed line are corresponding to the linear dynamic analysis using a standard FEM software. Here, the design basic wind pressure $w_0 = 0.5 \text{ kN/m}^2$, which corresponds to a design wind speed $V_h = 28.3 \text{ m/s}$, was assumed. At the same time, the distributed dead load was assumed to be 1.0 kN/m^2 .

As shown in Fig. 12, the nonlinear dynamic analysis results by the authors' program are well consistent in character with the results from linear dynamic analysis by the standard FEM software, which indicates the correctness of the theory and the program used in this paper. Moreover, the amplitude, or peak displacements obtained from the nonlinear dynamic time history analysis are obviously larger than that from linear analysis, especially at the vertex of shell in Z direction, which means that a nonlinear dynamic analysis considering large deformation of structures needs to be carried out for such type of structural system with certain flexibility.

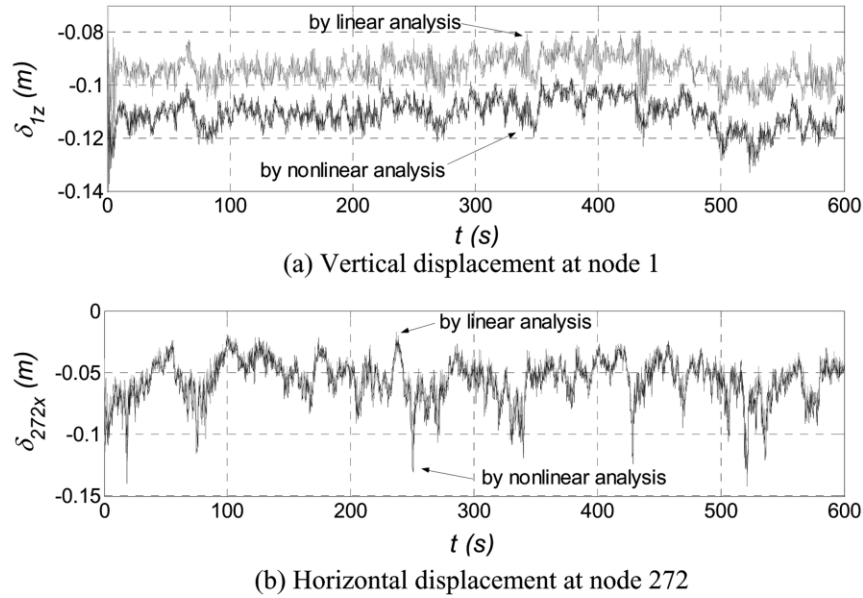


Fig. 12 Comparison between the nonlinear and the linear dynamic analysis results

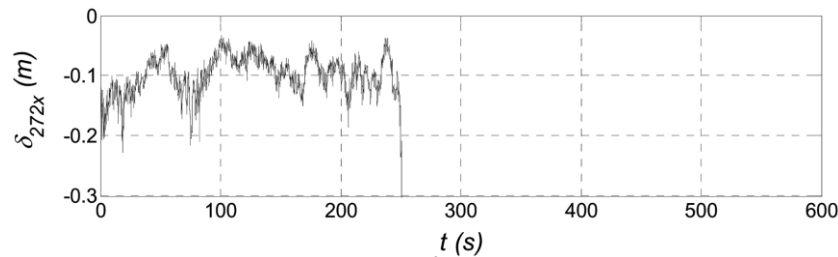


Fig. 13 Dynamic instability analysis

4.5. Dynamic instability analysis

With the above strategy and the corresponding program, dynamic stability can also be investigated conveniently through the characteristics of the equivalent current tangent stiffness matrix, and/or the divergence of the computation, and/or the maximum deformation during the nonlinear iterative analysis at each time step compared with the results from static instability analysis (Li and Shen 2001). Fig. 13 gives the results from dynamic stability analysis based on a proportional loading strategy, in which a dynamic instability has occurred at 250.5s when the total loading incremental factor, λ , was near to 10.0, i.e., $\lambda_{cr} = 10.0$. Generally speaking, dynamic stability analysis is an effective way to check the effect of wind load on the stability of single-layer reticulated shells. However, this kind of numerical analysis is a very time-consuming job, and only suitable for final analysis.

5. Conclusions

For single-layer reticulated shells, as well as other large-span spatial structural systems, nonlinear dynamic analysis considering large deformation for wind-induced vibration is necessary to be carried out in some cases. In this paper, based on a comparison between nonlinear static and dynamic analysis strategies, a practical framework for nonlinear dynamic time-history analysis considering dynamic stability problems for single-layer reticulated shells was introduced. On the help of the information of the wind pressure distribution on the surface of shells obtained from the wind tunnel tests, time-series data of the wind loads at each node of the structures were generated based on the proper orthogonal decomposition (POD) method. Using A K6-12 single-layer reticulated spherical shell as an example, nonlinear wind-induced vibration analysis was conducted. Compared with linear time-history analysis results, the efficiency of the strategy and the corresponding program was established. Furthermore, the necessity of nonlinear analysis for wind induced vibration of large-span single-layer reticulated shells has been shown. With the strategy and the corresponding program, dynamic instability problem could be investigated conveniently, although it is a time-consuming job, which means such kind of analysis is only suitable to be a final analysis in practical structural design processes.

References

- Abedi, K. and Habashizadeh, M., "Investigation in to the dynamic instability behavior of three dimension industrial space structures subjected to the finite duration and step impulsive loading", *Proc. of the Fifth Int. Conf. on Space Structures*, Guildford, UK, 929-938.
- Chresciewski, J. and Schmiot, R. (1985), "A solution control method for nonlinear finite element post-buckling analysis of structures", *Post-Buckling of Elastic Structures Proceeding of the Euromech Colloquium*, Edited by Z.S. Gaspar.
- Gioncu, V. (1995), "Buckling of reticulated shells: state-of-the-art", *Int. J. Space Struct.*, **10**, 1-46.
- Li, Y.Q. (2002), "Discussion on dynamic coefficients for wind-resistant design in single-layer reticulated shells", *Advances in Building Technology*, Anson, M., Ko, J.M. and Lam, E.S.S., editors, 1123-1130.
- Li, Y.Q., Shen, Z.Y. and Gu, X.L. (1997), "A study of tracing techniques for equilibrium paths including limit point and bifurcation point in nonlinear stability analysis", *Proc. the Seventh Int. Conf. on Computing In Civil And Building Engineering*, **1-4**, 249-254.
- Li, Y.Q., Tamura, Y., Yoshida, A. and Katsumura, A. (2002), "Wind modeling in BLWT and discussion on several problems", *Int. Conf. on Advances in Building Technology*, Hong Kong, China, 1131-1138.
- Li, Z.X. and Shen, Z.Y. (2001), "Shaking table tests of two shallow reticulated shells", *Int. J. Solids and Struct.*, **38**, 7875-7884.
- Oran, C. (1973), "Tangent stiffness in space frames", *J. Eng. Mech., ASCE*, **99-6**, 987-1001.
- Solari, G. (1990), "Generalized definition of gust factor", *J. Wind Eng. Ind. Aerodyn.*, **36**, 539-548.
- Tamura, Y., Suganuma, S., Kikuchi, H. and Hibi, K. (1999), "Proper orthogonal decomposition of random wind pressure field", *J. Fluids and Struct.*, **13**, 1069-1095.
- Uematsu, Y., Kuribara, O., Yamada, M., Sasaki, A. and Hongo, T. (2001), "Wind-induced dynamic behavior and its load estimation of a single-layer latticed dome with a long span", *J. Wind Eng. Ind. Aerod.*, **89**(14-15), 1671-1687.
- Uematsu, Y., Sone, T., Yamada, M. and Hongo, T. (2002), "Wind-induced dynamic response and its load estimation for structural frames of single-layer latticed domes with long spans", *Wind and Struct., An Int. J.*, **5**(6), 543-562.
- Uematsu, Y., Yamada, M., Inoue, A. and Hongo, T. (1997), "Wind loads and wind-induced dynamic behavior of a single-layer latticed dome", *J. Wind Eng. Ind. Aerod.*, **66**(3), 227-248.
- Von Karman, T. (1948), "Progress in the statistical theory of turbulence", *Proc. National Academy of Science*,

Washington DC, 530-539.

Xie, J.M., Irwin, P.A., Kilpatrick, J., Conley, G. and Soligo, M. (2000), "Determination of wind loads on large roofs and equivalent gust factors", *First Int. Symp. on Wind and Structures for the 21st Century*, Choi, Solari, Kanda & Kareem, Eds., Techno Press, Seoul, 417-424.

CC